Structure of Hexafluoroisopropanol–Water Mixtures by Molecular Dynamics Simulations

Toshio Yamaguchi[a,b], Shinya Imura[a], Tadashi Kai[a], and Koji Yoshida[a]

[a] Department of Chemistry, Fukuoka University, Jonan, Fukuoka 814-0180, Japan
[b] Advanced Materials Institute, Fukuoka University, Jonan, Fukuoka 814-0180, Japan

Reprint requests to T. Y.; E-mail: yamaguch@fukuoka-u.ac.jp

Z. Naturforsch. **68a,** 145 – 151 (2013) / DOI: 10.5560/ZNA.2012-0100
Received September 29, 2012 / published online February 15, 2013

Dedicated to Professor Alfred Klemm's 100th birthday

The structure of aqueous mixtures of 1,1,1,3,3,3-hexafluoro-propane-2-ol (HFIP) has been investigated at an alcohol mole fraction (x_{HFIP}) of 0.1, 0.2, and 0.4 by molecular dynamics (MD) simulation. The simulated pair correlation functions were compared with those obtained by empirical potential structure refinement (EPSR) modelling combined with neutron diffraction with isotopic substitution experiment. It is demonstrated that microheterogeneities of HFIP and water clusters occur at $x_{HFIP} = 0.1$ and 0.2 and that the tetrahedral-like structure of water is mostly disrupted at $x_{HFIP} = 0.4$. The evolution of the microscopic structure of the water–water, alcohol–water, and alcohol–alcohol pairs with alcohol concentration is revealed in terms of pair correlation functions and discussed from the standpoint of hydrophilic and hydrophobic hydration.

Key words: MD Simulation; Hexafluoroisopropanol; Water; Microhetrogeneities; Hydration.

1. Introduction

Aqueous mixtures of various alcohols have drawn much attention both in fundamental science [1 – 4] and in application fields [5 – 10] since the balance between the hydrophilic and hydrophobic solute–solvent interactions affects various physicochemical properties and consequently many natural and industrial processes. One of the recent topics is alcohol-induced α-helix promotion of proteins in aqueous solution. In particular, 1,1,1,3,3,3-hexafluoro-propane-2-ol (HFIP), shown in Figure 1, is the most effective among the aliphatic alcohols in stabilizing the α-helical structure of proteins and peptides [11 – 13]. Hong et al. reported a circular dichroism (CD) study on melittin and β-lactoglobulin in aqueous mixtures of HFIP as well as small-angle X-ray scattering measurements of the solvents [11]. They found that the stabilization of the secondary structure of the proteins takes place at around 30%(v/v) HFIP (a mole fraction of alcohol $x_{HFIP} = 0.0671$), where the maximum aggregation of solvent clusters is observed. These results suggested that the extent of solvent clustering is a key for understanding the stabilization of the secondary structure of proteins as well as of anomalies observed in various physicochemical properties of aqueous mixtures of alcohols.

To reveal the structure of aqueous mixtures of HFIP at the molecular level, several experimental and theoretical works have been performed [14 – 17]. Raman and ^{13}C NMR spectroscopic measurements were made for aqueous mixtures of HFIP over the entire range of HFIP mole fractions [15]. The results suggested the formation of micelle-like assemblies with the fluoroalkyl groups as an inside core. Their detailed structure at the molecular level remained, however, unexplored. A first molecular dynamics (MD) simulation study was performed on a dilute system of 216 water molecules and one HFIP molecule [14]. The results showed that the hydrogen bonding is enhanced around the hydroxyl group. Fioroni et al. proposed an all-atom model of HFIP for use in MD simulations [16]. They used this model together with SPC water to perform MD simulations of aqueous mixtures of HFIP over the whole range of the HFIP mole fractions. The calculated thermodynamic properties of neat HFIP are in good agreement with the experimental data, except for the mixing enthalpies of the mixtures. They observed a tendency for HFIP to cluster in SPC water, which is in qualitative agreement with experimental obser-

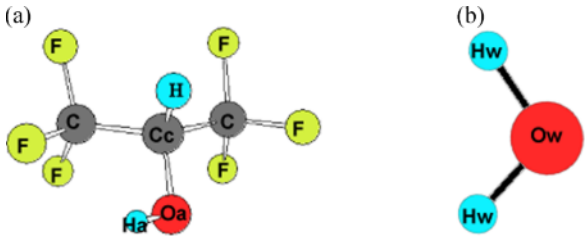

Fig. 1 (colour online). Molecular structure of HFIP (a) and water (b) with the atom labels.

Table 2. Generalized Amber Force Field Parameters for a HFIP molecule [20]. The symbols have their usual meanings. The atom labels are given in Figure 1.

Atom type	ε/kJmol^{-1}	σ/Å	q/e
F	0.2552	3.1181	−0.217
C	0.4577	3.3997	0.623
Cc	0.4577	3.3997	0.0639
H	0.07558	2.4714	0.104
Oa	0.7303	3.066	−0.550
Ha	0	0	0.439

vations [11]. However, the detailed structure of the water–water, HFIP–water, and HFIP–HFIP pairs at the molecular level was not reported.

The structural and dynamic properties of aqueous mixtures of HFIP were investigated over the entire range of HFIP mole fractions from comprehensive measurements with large-angle X-ray scattering (LAXS), small-angle neutron scattering (SANS), ^{19}F, ^{13}C, and ^{17}O nuclear magnetic resonance (NMR) chemical shifts, ^{17}O NMR relaxation, and mass spectrometry [17]. Overall, clustering and microheterogeneities are found to be most enhanced at $x_{\mathrm{HFIP}} \approx 0.1$, where a structural transformation of solvent clusters occurs from the tetrahedral-like structure of water to the neat structure of HFIP. However, the structural information obtained from LAXS and SANS is the sum of all pair correlation functions in a mixture, and thus the detailed structure of the individual water–water, HFIP–water, and HFIP–HFIP pairs remained unclear.

In the present study, we have performed MD simulations on aqueous mixtures of HFIP at $x_{\mathrm{HFIP}} = 0.1$, 0.2, and 0.4 at 298 K to reveal the detailed structural information on the water–water, HFIP–water, and HFIP–HFIP pairs at the molecular level. These mole fractions of HFIP were chosen because neutron diffraction experiments with isotopic substitution, combined with EPSR modelling, were available [18] and could be compared with the simulations.

2. MD Simulations

Periodic boxes with aqueous mixtures of HFIP with x_{HFIP} of 0.1, 0.2, and 0.4 were prepared. The important parameters of the periodic boxes are summarized in Table 1. The setup of the initial configuration and the subsequent energy minimization of each system in Table 1 were made with the EPSR package [19]. The pair potentials used were a generalized AMBER force field (GAFF) for HFIP [20] and TIP3P for water [21]. The parameter values of the GAFF potential are given in Table 2. The cutoff distance for the Lennard–Jones (LJ) part was 12 Å. The Ewald method was used to calculate the long-range Coulomb interactions. The SHAKE method was used to restrain the hydrogen atoms. Firstly, to equilibrate the systems, *NVT* simulations were run at 400 K for 200 ps, followed by cooling the system to 298 K and then simulations were run for another 300 ps. After this equilibration *NPT* simulations were run at 298 K for 1 ns, and the trajectory files were used for the structure analysis described in the next section. All simulations and trajectory analysis were performed using the AMBER11 software package [22]. Graphical drawings were made with the VMD software [23].

3. Results and Discussion

Figure 2 shows a comparison of the Ow–Ow pair correlation functions (PCFs) $g_{\mathrm{OwOw}}(r)$ of the water–water pairs for each of the solutions obtained by MD simulation with those derived from EPSR modelling combined with neutron diffraction with isotopic substitution (NDIS) experiments [18]. The simulated $g_{\mathrm{OwOw}}(r)$ PCFs are significantly higher in amplitude than those obtained by EPSR modelling. This difference in amplitude can be attributed to the so-called ex-

Table 1. Parameters for the periodic boxes for the MD simulations of aqueous mixtures of HFIP.

x_{HFIP}	N_{HFIP}	N_{w}	Cell lengths/Å	Density/g·cm^{-3}
0.1	100	900	34.20 × 32.85 × 33.84	1.261
0.2	200	800	38.09 × 37.57 × 37.17	1.380
0.4	400	600	40.71 × 40.48 × 39.86	1.496

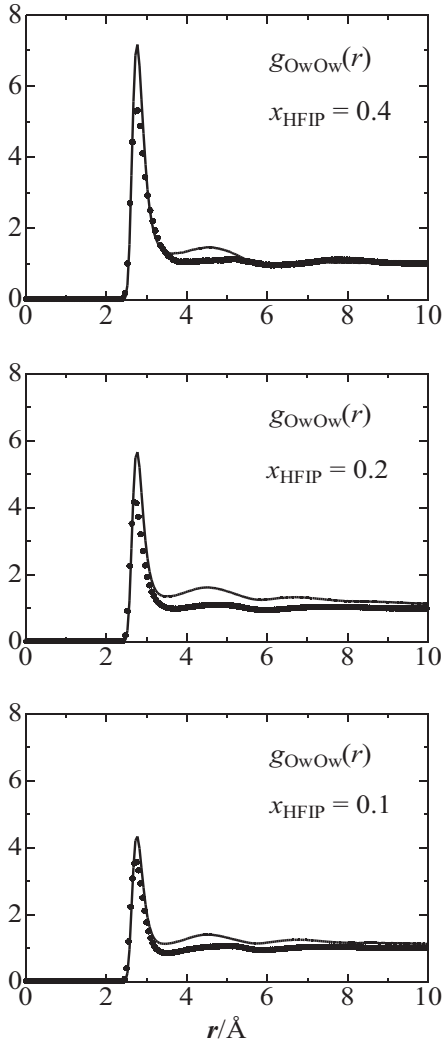

Fig. 2. Ow–Ow PCFs of the water–water pairs for the aqueous mixtures of HFIP at $x_{HFIP} = 0.1$, 0.2, and 0.4. The solid lines represent the simulated values obtained in this study and the circles represent those derived by EPSR modelling combined with NDIS experiments [22].

cluded volume effects [24, 25] which originate from the segregation of water molecules from the HFIP clusters. This result suggests that the present force fields for HFIP and water molecules tend to emphasize the water–water interactions. This can also be seen in the second peak centered at 4.5 Å, which is higher in amplitude in the simulated $g_{OwOw}(r)$ PCF. The positions of the first peaks are in good agreement with each other for the MD simulation and the EPSR modelling [18] for all solutions.

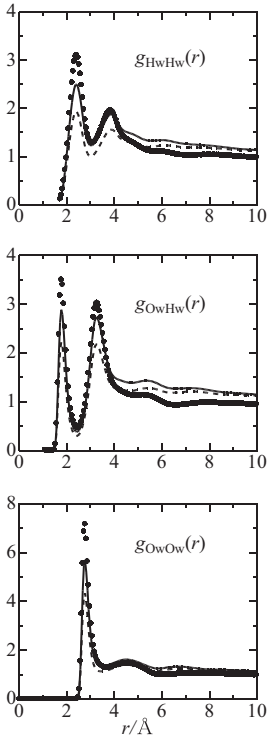

Fig. 3. Water–water PCFs for the aqueous mixtures of HFIP at $x_{HFIP} = 0.1$, 0.2, and 0.4. For each of the depicted PCFs, the dashed lines represent the 0.1 mole fraction of HFIP, the solid lines represent the 0.2 mole fraction of HFIP, and the dots represent the 0.4 mole fraction of HFIP.

3.1. Water–Water Pairs

Figure 3 shows the $g_{HwHw}(r)$, $g_{OwHw}(r)$, and $g_{OwOw}(r)$ PCFs for aqueous mixtures of HFIP at $x_{HFIP} = 0.1$, 0.2, and 0.4 obtained from the MD simulations. The first and second peaks in the three kinds of PCFs increase with increasing HFIP concentration. This increase of the peaks arises from the excluded volume effect, which comes from a rise in the local density at short distances due to the exclusion of water from the region occupied by HFIP molecules, i. e. the microheterogeneities between water and HFIP clusters in the solutions. It thus cannot be taken to indicate an increased water structure. The coordination numbers of Hw–Hw, Ow–Hw, and Ow–Ow are given for all solutions in Table 3. The coordination number of the Ow–Ow pairs are around four for the solutions at $x_{HFIP} = 0.1$ and 0.2, showing that the tetrahedral-like structure of water remains in these solutions. In contrast, the value in the solution at $x_{HFIP} = 0.4$ drops

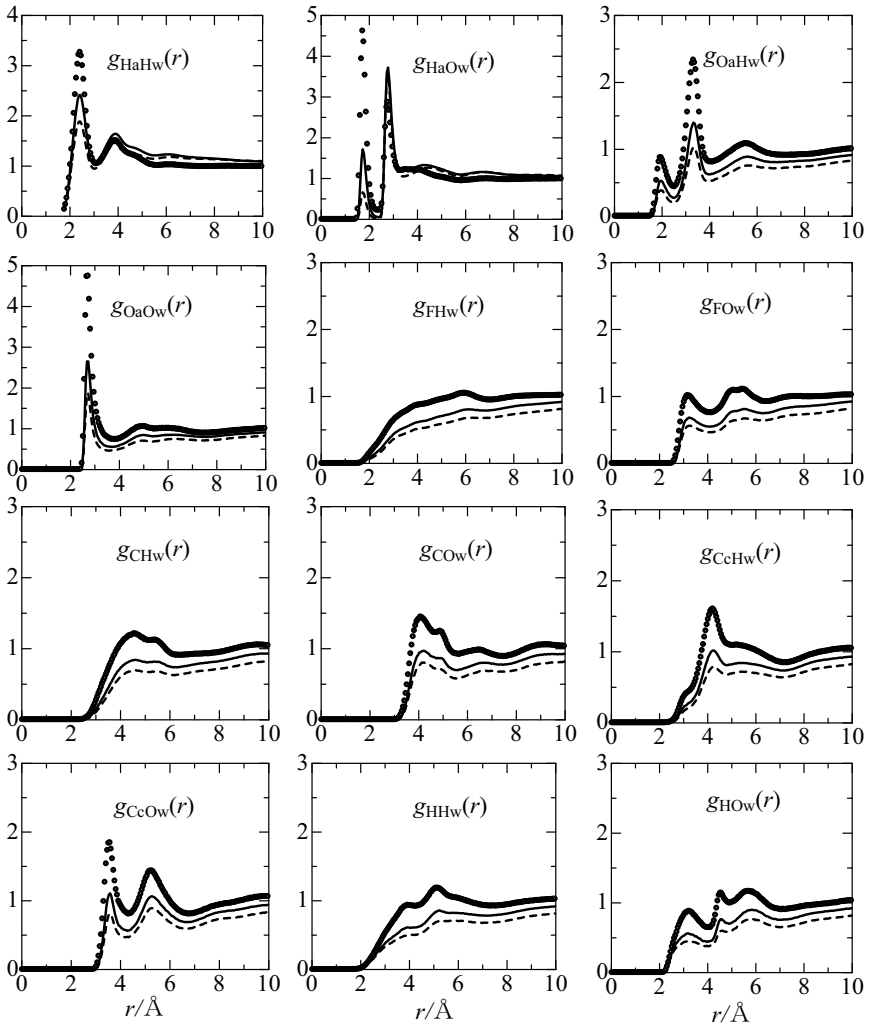

Fig. 4. HFIP–water PCFs for the aqueous mixtures of HFIP at $x_{\mathrm{HFIP}} = 0.1$, 0.2, and 0.4. For each of the depicted PCFs, the dashed lines represent the 0.1 mole fraction of HFIP, the solid lines represent the 0.2 mole fraction of HFIP, and the dots represent the 0.4 mole fraction of HFIP.

by a factor of two compared with those for the solutions at $x_{\mathrm{HFIP}} = 0.1$ and 0.2. This finding shows a disruption of the tetrahedral-like structure of water due to the inclusion of HFIP molecules into the structure of water. According to the previous LAXS and SANS studies [17], the structural transition of the solvent appeared at $x_{\mathrm{HFIP}} \approx 0.1$, which is not consistent with the composition estimated from the present MD simulation. As discussed in the previous section, this is probably because the water–water pairs are less perturbed by HFIP in the present simulation than expected from the NDIS study.

3.2. HFIP–Water Pairs

Figure 4 shows the HFIP–water PCFs for all the three HFIP mole fractions. The hydration structure around the hydroxyl group of a HFIP molecule can be seen from the $g_{\mathrm{HaHw}}(r)$, $g_{\mathrm{HaOw}}(r)$, $g_{\mathrm{OaHw}}(r)$, and $g_{\mathrm{OaOw}}(r)$ PCFs. All PCFs increase in amplitude with increasing HFIP concentration due to the excluded volume effect, as discussed in the previous sections. The peak at 1.8 Å for the $g_{\mathrm{HaOw}}(r)$ and $g_{\mathrm{OaHw}}(r)$ PCFs and that at 2.8 Å for the $g_{\mathrm{OaOw}}(r)$ PCFs show that hydrogen bonding occurs between the HFIP hydroxyl group

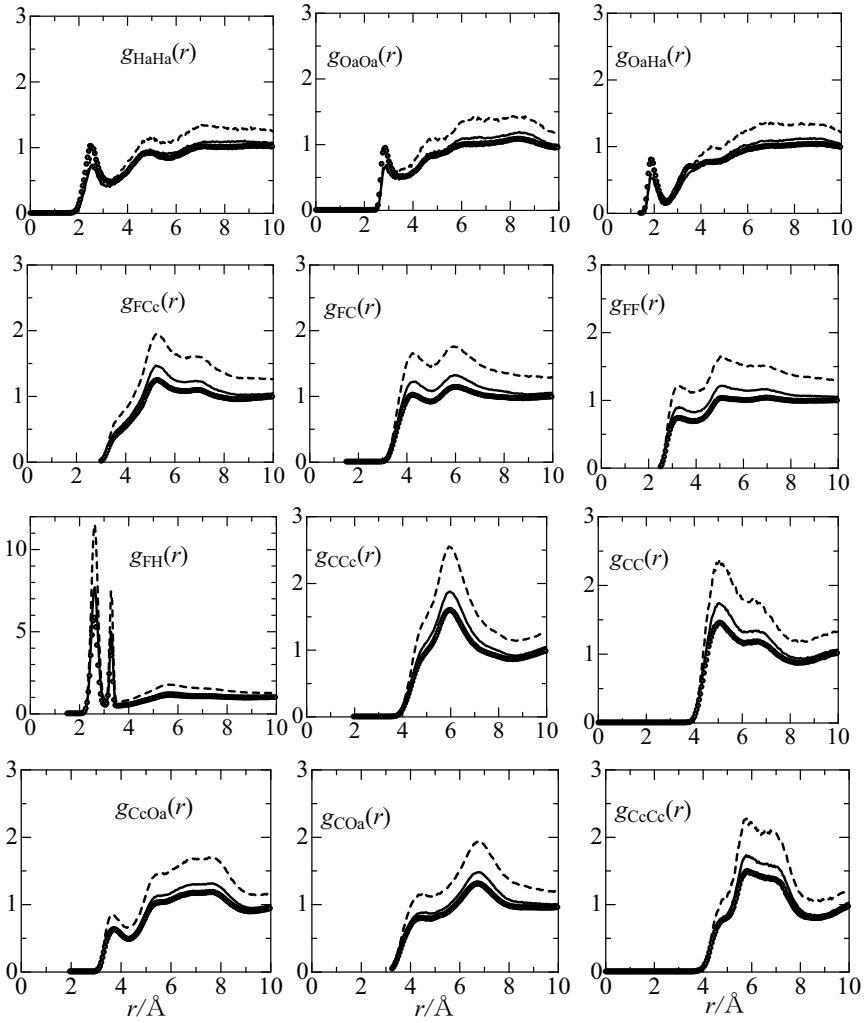

Fig. 5. HFIP–HFIP PCFs for the aqueous mixtures of HFIP at $x_{HFIP} = 0.1$, 0.2, and 0.4. For each of the depicted PCFs, the dashed lines represent the 0.1 mole fraction of HFIP, the solid lines represent the 0.2 mole fraction of HFIP, and the dots represent the 0.4 mole fraction of HFIP.

and water. The present results are in good agreement with those obtained in the previous study [16]. The more pronounced peak at 1.8 Å for the $g_{HaOw}(r)$ PCF than that for the $g_{OaHw}(r)$ PCF suggests that a HFIP molecule is preferable as a hydrogen bond acceptor.

The hydration structure around the CF_3 groups of HFIP can be seen from the $g_{FHw}(r)$, $g_{FOw}(r)$, $g_{CHw}(r)$, and $g_{COw}(r)$ PCFs in Figure 4. It has long been discussed whether or not some hydrogen bonding occurs between the CF_3 fluorine atom and water. As seen in the broad $g_{FHw}(r)$ PCFs, there are no strong orientational correlations between the fluorine and water-hydrogen atoms. However, a peak is observed at 3.0 Å in the $g_{FOw}(r)$ PCFs, which might correspond to the hydrogen-bond distance between the fluorine and water-oxygen atoms. These findings suggest that weak hydrogen bonds occur between the CF_3 group and water. As seen in Table 3, the coordination numbers of the F–Ow and C–Ow pairs decease monotonously with increasing HFIP concentration, and there is no sharp decrease in the coordination number of these pairs, as found in the water–water pairs described in the previous section. Thus, the hydration structure around the CF_3 group is less perturbed with increasing solute con-

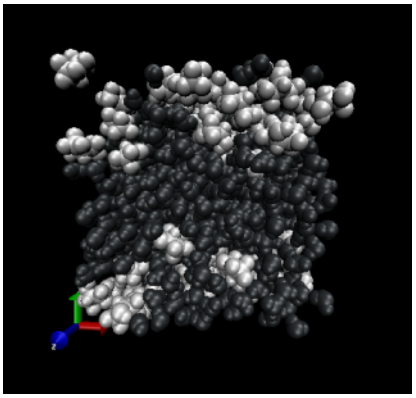

x_{HFIP}=0.1

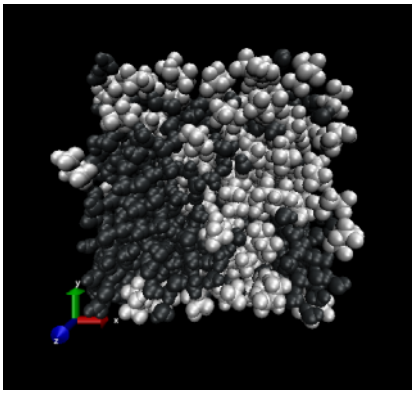

x_{HFIP}=0.2

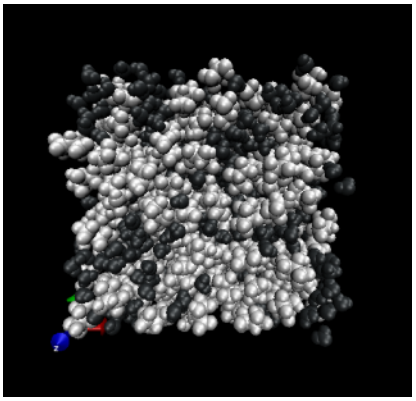

x_{HFIP}=0.4

Fig. 6 (colour online). Snapshots of the simulation boxes after 1 ns run for the aqueous mixtures of HFIP at $x_{HFIP} = 0.1$ (top frame), 0.2 (center frame), and 0.4 (bottom frame). The white balls represent HFIP molecules and the black balls represent water molecules.

Table 3. Coordination numbers for the water–water, HFIP–water, and HFIP–HFIP pairs for the aqueous mixtures of HFIP with mole fractions $x_{HFIP} = 0.1$, 0.2, and 0.4. r_{max} is the upper limit of integration of the individual PCFs.

Atom Pair	r_{max}	$x_{HFIP} = 0.1$	$x_{HFIP} = 0.2$	$x_{HFIP} = 0.4$
Ow–Hw	2.42	1.9	1.8	1.5
Ow–Ow	3.42	4.3	3.8	2.2
Oa–Hw	2.47	0.3	0.3	0.2
Oa–Ow	3.62	2.1	1.9	1.6
Oa–Ha	2.52	1.0	1.0	1.1
F–Ow	4.02	1.8	1.5	1.1
C–Hw	6.37	11.9	9.6	6.9
C–Ow	4.72	3.7	3.1	2.3
Cc–Hw	4.77	4.1	3.5	2.8
Cc–Ow	4.27	2.2	1.9	1.6
C–C	6.27	3.1	3.5	4.0
C–F	4.97	2.1	2.3	2.4
F–F	3.97	1.1	1.2	1.2
Cc–Cc	8.62	8.5	9.7	11.6

centration than that of the hydroxyl groups of a HFIP molecule.

3.3. HFIP–HFIP Pairs

Figure 5 shows the HFIP–HFIP PCFs for all solutions. The $g_{OaHa}(r)$ and $g_{OaOa}(r)$ PCFs have peaks at 1.8 and 2.8 Å, respectively, showing that some hydrogen bonding occurs between HFIP molecules. The coordination numbers of the Oa–Ha and Oa–Oa pairs in Table 3 show no significant change with HFIP concentration. This also indicates that there are no strong hydrogen bonds between HFIP molecules, probably due to the bulky CF_3 groups. This is in good agreement with previous findings [16]. Instead, the coordination numbers of the C–C and Cc–Cc pairs increase with increasing HFIP mole fraction. However, there is no specific increase in the coordination number with solute concentration: there are about $8 \sim 12$ HFIP molecules around a central HFIP molecule. Judging from the present results, HFIP molecules tend to cluster in such a fashion that the fluoroalkyl groups assemble as an inside core with the hydroxyl groups facing outward to form hydrogen bonds with the surrounding water molecules [15].

In Figure 6, snapshots of the simulation boxes of the three aqueous mixtures of HFIP are shown. The microhetrogeneities of water and HFIP clusters are characteristic at the HFIP mole fractions of 0.1 and 0.2, whereas the water clusters are mostly disrupted in the

solution with a HFIP mole fraction of 0.4, as seen in the PCFs.

4. Conclusions

MD simulations have been performed at 298 K for aqueous mixtures of HFIP at $x_{HFIP} = 0.1$, 0.2, and 0.4. From a comparison of the simulated Ow–Ow PCFs with those obtained from EPSR simulations combined with NDIS experiments, the present force fields for HFIP and water tend to stabilize the water–water pairs more strongly than expected from the NDIS study. Microheterogeneities between water and HFIP molecules occur at $x_{HFIP} = 0.1$ and 0.2. The tetrahedral-like network structure of water is disrupted at $x_{HFIP} = 0.4$, which is higher than the composition estimated from the previous LAXS and SANS study, due probably to the force fields employed. Strong hydrogen bonds are formed between HFIP and water. Furthermore, the hydrogen bonding between HFIP molecules is weaker than that between HFIP and water molecules. Hydrogen bond-type configurations appear between the CF_3-fluorine atom and water without strongly preferred orientation.

Acknowledgements

This work was supported in part by MEXT (15076211, 17550023, and 16GS0417), a High-Tech Research Center Project (2005∼2007) of Fukuoka University, and funds (065005, 095004, and 125004) from the Central Research Institute of Fukuoka University. The calculations were made in part on the High Performance Application Server of Kyushu University.

[1] N. Nishi, S. Takahashi, M. Matsumoto, A. Tanaka, K. Muraya, T. Takamuku, and T. Yamaguchi, J. Phys. Chem. **99**, 462 (1995).
[2] D. T. Bowron, J. L. Finney, and A. K. Soper, J. Phys. Chem. B **102**, 3551 (1998).
[3] T. Yamaguchi, Pure Appl. Chem. **71**, 1741 (1999).
[4] T. Takamuku, T. Yamaguchi, M. Asato, M. Matsumoto, and N. Nishi, Z. Naturforsch. **55a**, 513 (2000).
[5] M. Buck, H. Schwalbe, and C. M. Dobson, J. Mol. Biol. **257**, 669 (1996).
[6] H. Lu, M. Buck, S. E. Radford, and C. M. Dobson, J. Mol. Biol. **265**, 112 (1997).
[7] S. Kumaran and R. P. Roy, J. Peptide Res. **53**, 284 (1999).
[8] F. Khan, R. H. Khan, and S. Muzammil, Biochim. Biophys. Acta **1481**, 229 (2000).
[9] R. Stoll, W. Voelter, and T. A. Holak, Biopolymers **41**, 623 (1997).
[10] N. Hirota-Nakaoka and Y. Goto, Bioorg. Med. Chem. **7**, 67 (1999).
[11] D. Hong, M. Hoshino, R. Kuboi, and Y. Goto, J. Am. Chem. Soc. **121**, 8427 (1999).
[12] T. Fujinaga, S. Nakamura, S. Krishtal, K. Yoshida, S. Lee, K. Kanazawa, T. Nemoto, and T. Yamaguchi, Fukuoka Univ. Sci. Rep. **37**, 23 (2007).
[13] K. Yoshida, J. Kawaguchi, S. Lee, and T. Yamaguchi, Pure Appl. Chem. **80**, 1337 (2008).
[14] K. Kinugawa and K. Nakanishi, J. Chem. Phys. **89**, 5834 (1988).
[15] Y. Mizutani, K. Kamogawa, T. Kitagawa, A. Shimizu, Y. Taniguchi, and K. Nakanishi, J. Phys. Chem. **95**, 1790 (1991).
[16] M. Fioroni, K. Burger, A. E. Mark, and D. Roccatano, J. Phys. Chem. B **105**, 10967 (2001).
[17] K. Yoshida, T. Yamaguchi, T. Adachi, T. Otomo, D. Matsuo, T. Takamuku, and N. Nishi, J. Chem. Phys. **119**, 6132 (2003).
[18] K. Yoshida, T. Yamaguchi, D. T. Bowron, and J. L. Finney, J. Neutron Research **12**, 305 (2004).
[19] EPSR17: The latest version is available at the following web page: http://www.isis.rl.ac.uk/Disordered/dmgroup_home.htm.
[20] J. Wang, R. M. Wolf, J. W. Caldwell, P. A. Kollman, and D. A. Case, J. Comput. Chem. **25**, 1157 (2004).
[21] M. W. Mahoney and W. L. Jorgensen, J. Phys. **112**, 8910 (2000).
[22] D. A. Case, T. A. Darden, T. E. Cheatham, III, C. L. Simmerling, J. Wang, R. E. Duke, R. Luo, R. C. Walker, W. Zhang, K. M. Merz, B. Roberts, B. Wang, S. Hayik, A. Roitberg, G. Seabra, I. Kolossvai, K. F. Wong, F. Paesani, J. Vanicek, J. Liu, X. Wu, S. R. Brozell, T. Steinbrecher, H. Gohlke, Q. Cai, X. Ye, J. Wang, M.-J. Hsieh, G. Cui, D. R. Roe, D. H. Mathews, M. G. Seetin, C. Sagui, V. Babin, T. Luchko, S. Gusarov, A. Kovalenko, and P. A. Kollman, AMBER 11, University of California, San Francisco 2010.
[23] W. Humphrey, A. Dalke, and K. Schulten. J. Mol. Graphics. **14**, 33 (1996).
[24] A. K. Soper, J. Phys. Condens. Matter **9**, 2399 (1997).
[25] A. K. Soper, F. Bruni, and M. A. Ricci, J. Chem. Phys. **109**, 1486 (1998).